Springer

Journal of Mechanical Science and Technology 23 (2009) 2125~2137

Journal of Mechanical Science and Technology

www.springerlink.com/content/1738-494x
DOI 10.1007/s12206-009-0623-x

Analysis of the nonlinear behavior of gear pairs considering hydrodynamic lubrication and sliding friction †

Cheon Gill-Jeong

Division of Mechanical Engineering, Wonkwang University, Iksan City, Jeon-Buk, 570-749, Korea

(Manuscript Received August 12, 2008; Revised February 7, 2009; Accepted April 21, 2009)

Abstract

This paper describes an analysis of the nonlinear behavior of gear pairs according to the direct contact elastic deformation model over a wide range of speeds, considering the hydrodynamic effects and friction force. The inclusion of the hydrodynamic effect facilitates nonlinearity by increasing the overlap range (*i.e.*, multiple solution regimes) and damping, as well as decreasing elastic deformation and tooth reaction forces. The effects of various lubrication parameters, such as viscosity and film width, on the nonlinear dynamic behavior were analyzed. While the viscosity has a strong effect on the behavior of gear pair systems, friction has very little effect on torsional behavior. Although the model of direct contact without friction has overall nonlinear behavior similar to the model including hydrodynamic effects with friction, the time data of these models are different due to the squeeze effect.

Keywords: Gear pair; Hydrodynamic lubrication; Nonlinear behavior; Sliding friction; Squeeze effect

1. Introduction

Many previous studies regarding the dynamic behavior of gear pairs have been based on modeling tooth contact as a spring and damper system, with the stiffness of the equivalent spring based on elastic deformation, such as Hertzian deformation or tooth bending. However, there has been little research into the effects of sliding friction or the hydrodynamic forces on the dynamic behavior of gear pairs.

Vaishya and Singh [1, 2] used the direct-contact model with Coulomb friction between gear teeth, and reported that friction has only a minimal effect on the torsional instabilities of the dynamic gear system. They investigated the dynamic effects of friction-induced nonlinearity using both linear and nonlinear time-varying systems and showed that friction is capable of reducing large oscillations under certain resonant conditions.

He et al. [3, 4] studied the effects of sliding friction on the dynamics of a spur gear pair using finite element analysis to compute the mesh stiffness at each time point. They concluded that the main effect of sliding friction is enhancement of the dynamic transmission error (DTE) magnitude at the second gear mesh harmonic, and that the sliding friction forces primarily excite the off-line of action (OLOA) motion.

Howard et al. [5] presented a dynamic model with tooth torsional mesh stiffness developed by finite element analysis, which included sliding friction and a single tooth crack as a diagnostic technique. They showed that in most cases, the effect of friction modeled using Coulomb friction produced a negligible change in the resulting kurtosis values.

Velex and Sainsot [6] analyzed the linear dynamic behavior of gear pairs considering Coulomb friction, and found that tooth friction appears as a non-negligible excitation source for translation, and that the torsional response is less sensitive to tooth friction than the bending response. They used a stiffness

† This paper was recommended for publication in revised form by Associate Editor Eung-Soo Shin

* Corresponding author. Tel.: +82 63 851 6686, Fax.: +82 63 850 6691
E-mail address: gjcheon@wku.ac.kr

model based on contact deformation and structural deflection of gear teeth.

Most of the research on gear dynamics uses tooth stiffness based on tooth deformation by direct solid contact. Some studies have modeled the tooth stiffness as a constant through the complete tooth contact period with a piecewise nonlinear function, assuming that the contact reaction force between the teeth is zero when they are separated from each other.

However, as almost all gear systems are operated under fluid lubrication, a reaction force between the teeth due to the squeeze film effect will occur even when the two solid surfaces are not in contact. Therefore, it seems reasonable to consider the elastohydrodynamic lubrication effect between contacting teeth in analysis of the dynamic behavior of gear pair systems. Blankenship and Kahraman [7] showed that a gear pair does not always maintain contact and tooth separation does occur. Hence, a mixed model including a hydrodynamic contact regime as well as a direct-contact regime for the tooth reaction force is necessary.

Several previous reports [8-10] have described the elastohydrodynamic effects on gear systems as functions of the pressure distribution, minimum film thickness, and friction coefficients. However, the analysis models in these studies were limited to static conditions that included only a specific single pair of teeth.

There have been very few investigations of the dynamic behavior of gear pair systems considering the elastohydrodynamic lubrication effect between teeth. Theodossiades et al. [11, 12] studied idle gear rattling phenomena in vehicular transmissions, taking into account the effect of lubrication. They treated gear impact surfaces as lubricated conjunctions rather than the more frequently reported dry impacting solids. They examined the influence of lubrication on the torsional vibration of lightly loaded idling gears, and showed that the lubrication film behaves as a time-varying nonlinear spring/damper element. They calculated the lubrication stiffness by differentiating the lubricant reaction force with respect to the film thickness, assuming full lubrication and that squeeze film terms were negligible. They found that the lubricant properties significantly affected the system response, and showed that the viscosity is one of the main factors governing the overall system behavior.

Brancati et al. [13, 14] proposed an analytical model that accounts for the oil squeeze effect between the impacting teeth of mating gears based on the influence of the oil-damping effects on dynamic behavior of the automotive idle rattle phenomenon. Unlike the approach taken by other researchers, they modeled the interaction force between the teeth in three phases. When the distance between the flanks was less than zero, the meshing stiffness was calculated due to elastic deformation of the teeth in contact, as in models used in most other research. They included the contact phase of the elastohydrodynamic lubrication regime when the distance was greater than average surface roughness (h_{min}) of the tooth flank surfaces. The third phase was when the distance was positive but less than h_{min}; there, the damping force was assumed to be a constant saturation value. With this model, they showed that the presence of the oil reduces the number and intensity of impacts between the teeth, and contributes to reduction of rattling.

However, Brancati et al. did not include an entraining term, and calculated the hydrodynamic force counting only one tooth pair contact, while the direct contact force was calculated considering the equivalent stiffness of one or two tooth pairs according to the meshing phase. They did not analyze the nonlinear behavior, such as jump phenomena of a gear pair system over a wide range of speeds.

Here, the author reports an analysis of the nonlinear behavior of a gear pair system over a wide range of speeds based on a modified analysis model that considers the hydrodynamic effect and friction, as well as the effects of various parameters, such as lubricant viscosity and friction coefficient.

2. Mathematical model

The system in this study consisted of two gears mounted on well-aligned input and output shafts (Fig. 1). The gears were standard errorless involute spur gears with no modifications, and the gear pair was modeled as a purely torsional vibration system. The gears were assumed to be fully lubricated by Newtonian lubricant, and shear force was ignored. For simplicity of calculation, the conditions of isothermal incompressibility and constant viscosity were assumed. The torque and speed of the input shaft were assumed to be constant.

The equations of motion of the two gears were as follows:

$$\begin{aligned} T_d - T_{mp} &= I_p \ddot{\theta}_p \\ T_{mg} - T_o &= I_g \ddot{\theta}_g \end{aligned} \tag{1}$$

where

$$T_{mp}=\begin{Bmatrix}F_{en}r_p-T_{efp},\ \left|r_p\theta_p-r_g\theta_g\right|\geq b\\ F_{hn}r_p-T_{hfp},\ \left|r_p\theta_p-r_g\theta_g\right|\prec b\end{Bmatrix},$$
$$T_{mg}=\begin{Bmatrix}F_{en}r_g-T_{efg},\ \left|r_p\theta_p-r_g\theta_g\right|\geq b\\ F_{hn}r_g-T_{hfg},\ \left|r_p\theta_p-r_g\theta_g\right|\prec b\end{Bmatrix}, \quad (2)$$

$$F_{en}=k(t)(r_p\theta_p-r_g\theta_g)+c(r_p\dot{\theta}_p-r_g\dot{\theta}_g) \quad (3)$$

T_d and T_o are the static driving and load torques, while T_{mp} and T_{mg} are torques due to tooth meshing forces by the pinion and gear, respectively. The pinion and gear have base circle radii r_p and r_g, and mass moments of inertia of I_p and I_g, respectively. The total backlash is $2b$, and parameters θ_p and θ_g represent the vibrations of the gears about the nominal rigid body rotation. The forces F_{en} and F_{hn} are normal forces acting along the line of action (LOA) due to elastic deformation and the hydrodynamic effect, respectively. F_{en} was calculated by using the dry contact model used in previous research [15-17] (details not shown here). The contacting teeth were regarded as a spring and damper, where k (t) is the time-varying mesh stiffness obtained by assuming a rectangular wave. F_{hn} consists of the squeeze term (F_{hs}) and the entraining term (F_{he}). The moment arms of the normal forces F_{en} and F_{hn} are always equal to the base radius.

T_{efp} and T_{hfp} are the torques acting on the pinion induced by the direct contact friction force F_{ef} and the hydrodynamic friction force F_{hf}, respectively. T_{efg} and T_{hfg} are the torques acting on the gear induced by the direct contact friction force F_{ef} and the hydrodynamic friction force F_{hf}, respectively.

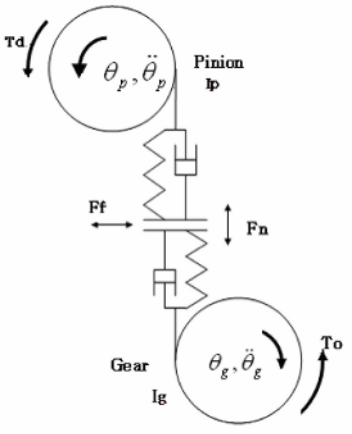

Fig. 1. Schematic diagram of gear pairs.

The general Reynolds equation was used to calculate the hydrodynamic normal force F_{hn} [18].

$$\frac{\partial}{\partial x}\left(\frac{\rho h^3}{12\eta}\frac{\partial p}{\partial x}\right)+\frac{\partial}{\partial y}\left(\frac{\rho h^3}{12\eta}\frac{\partial p}{\partial y}\right)=\frac{\partial}{\partial x}\left[\frac{\rho h(u_a+u_b)}{2}\right]+\frac{\partial}{\partial y}\left[\frac{\rho h(v_a+v_b)}{2}\right]+\frac{\partial(\rho h)}{\partial t} \quad (4)$$

By neglecting side leakage and assuming that the fluid is incompressible and isoviscous, Eq. (4) reduces to

$$\frac{\partial}{\partial\xi}\left(h^3\frac{\partial p}{\partial\xi}\right)=12\eta_o\bar{u}\frac{\partial h}{\partial\xi}+12\eta_o\frac{\partial h}{\partial t} \quad (5)$$

$$\bar{u}=\frac{u_p+u_g}{2} \quad (6)$$

where h is the film thickness, η_o is an ambient dynamic viscosity, and $\bar{u}$ is an equivalent entraining velocity assumed to constant along the ξ-direction (Fig. 2). Parameters u_p and u_g are the surface tangential velocities of gear pairs at the meshing point.

Assuming full lubrication, the film thickness is equal to the distance between the two flanks as a function of ξ due to the flank curvature, and is expressed as follows [18, 19]

$$h=x+\frac{\xi^2}{R} \quad (7)$$

where x is the minimum distance between two flanks at ξ = 0. Parameter x and the DTE are defined as

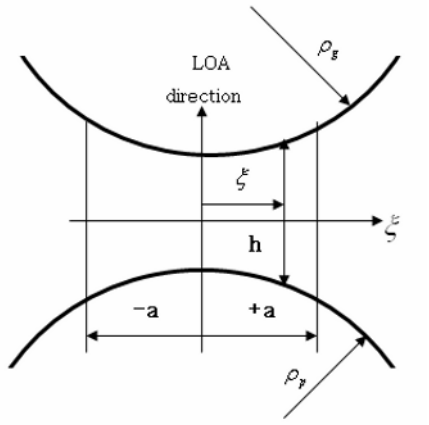

Fig. 2. Lubricant film parameters.

$$x = b - DTE,$$
$$DTE = r_p\theta_p - r_g\theta_g \tag{8}$$

where 2*b* is the total backlash. The equivalent radius of the contacting point *R* is defined as

$$R = 2\left(\frac{\rho_p\rho_g}{\rho_p + \rho_g}\right) \tag{9}$$

where ρ_p and ρ_g are the pinion and gear tooth surface radii of curvature in the transverse plane, respectively.

By integrating Eq. (5) twice with these boundary conditions

$$p = 0,\ \xi = -a, a$$
$$\frac{\partial p}{\partial \xi} = 0,\ \xi = 0 \tag{10}$$

the pressure was derived in this study as

$$p(\xi) = 3\eta_o R^3\dot{x}\left[\frac{1}{(a^2+Rx)^2} - \frac{1}{(\xi^2+Rx)^2}\right] + 12\eta_o\bar{u}R^2\left[\begin{array}{l}\dfrac{a(a^2-Rx)}{8Rx(Rx+a^2)^2} + \dfrac{\xi(\xi^2-Rx)}{8Rx(Rx+\xi^2)^2} + \\ \dfrac{1}{8(Rx)^{\frac{3}{2}}}\left\{acrtg\left(\dfrac{a}{\sqrt{Rx}}\right) + arctg\left(\dfrac{\xi}{\sqrt{Rx}}\right)\right\}\end{array}\right] \tag{11}$$

where the first and second terms on the right-hand side are due to squeeze and entraining terms, respectively.

By integrating the pressure equation along the film width (-*a*, *a*), the hydrodynamic force due to the lubrication film between separated tooth flanks can be defined as

$$F_{hn} = \frac{3\eta_o w R^{\frac{1}{2}}(a\bar{u} - R\dot{x})}{x^{\frac{3}{2}}(a^2+Rx)^2}\left[\begin{array}{l}a(a^2-Rx)\sqrt{Rx} + \\ (a^2+Rx)^2 arctg\left(\dfrac{a}{\sqrt{Rx}}\right)\end{array}\right] \tag{12}$$

where *w* is the face width. Considering the roughness of the tooth flank surfaces (h_{min}), the hydrodynamic force is assumed to be saturated when the distance between the flanks is positive but less than h_{min} [13]. The total hydrodynamic force must be calculated by summation when two pairs of teeth come into contact. A negative value of $\dot{x}$ indicates a recession of the meshing gear teeth with each other, which does not contribute to the hydrodynamic force.

The tooth surface radii of curvature ρ_p and ρ_g are expressed as

$$\rho_p = (r_p\tan\phi - s_p) + s$$
$$\rho_g = (r_g\tan\phi + s_p) - s \tag{13}$$

where ϕ is the pressure angle. In Fig. 3, the LOA is from *A* to *B*. *L*, *P*, and *H* are the lowest point of single-tooth contact (LPSTC), the pitch point, and highest point of single-tooth contact (HPSTC), respectively, and *s* is the distance from the starting point (*A*) to the contact point (*C*) along the LOA.

To synchronize the time-varying stiffness with the tooth meshing phase, the distance of the contact point (*s*) is expressed as a function of time (Fig. 4). As the magnitude of *s* varies periodically with the tooth mesh frequency f_m, it can be Fourier-transformed and expressed as shown in Eq. (14) with *L* = 30. τ_m is the tooth mesh cycle.

$$s(t) = \frac{p_b}{2} - \frac{p_b}{\pi}\sum_{i=1}^{L}\frac{1}{i}\sin(i2\pi f_m t) \tag{14}$$

When the new tooth pair comes into contact while the old tooth pair is still in contact (*i.e.*, $s \le s_l$), the radii of curvature of the old contact teeth are

$$\rho_{p,old} = r_p\tan\phi + (s + s_h - s_p) = \rho_p + s_h$$
$$\rho_{g,old} = r_g\tan\phi - (s + s_h - s_p) = \rho_g - s_h \tag{15}$$
$$s_h = p_b = \pi m\cos\phi$$

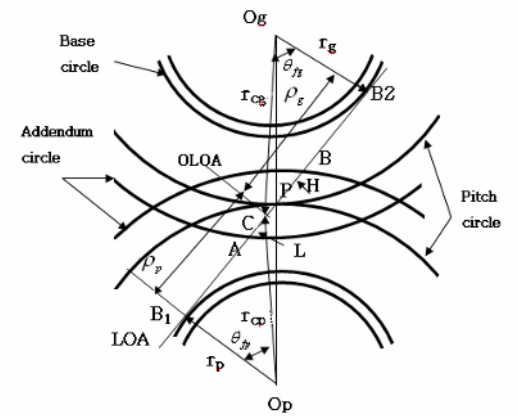

Fig. 3. Contact area parameters.

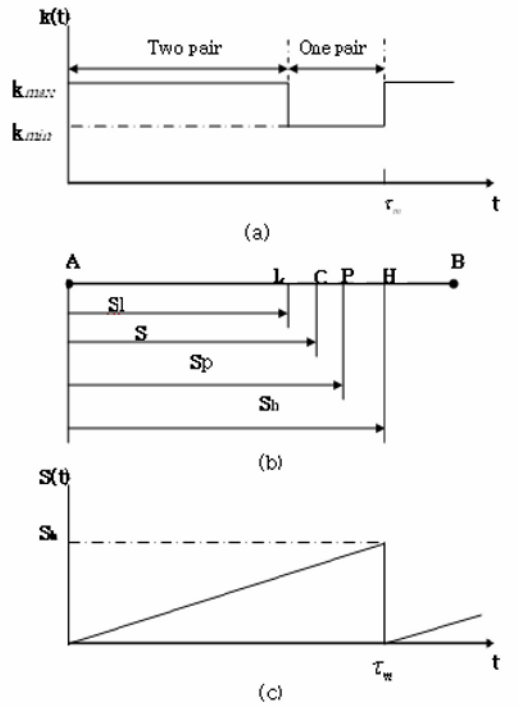

Fig. 4. Mesh stiffness and LOA: (a) rectangular type mesh stiffness (b) distance from starting point A along the LOA (c) distance as a function of time per tooth mesh cycle.

where p_b is the transverse base pitch and m is the module.

The entraining velocities, u_p and u_g, are

$$u_p = \frac{\pi N_p}{30}\rho_p,\ u_g = \frac{\pi N_g}{30}\rho_g\ , \tag{16}$$

where N_p and N_g are the numbers of teeth in the pinion and gear, respectively.

The direct contact Coulomb friction force F_{ef} is expressed as

$$F_{ef} = \mu F_{en}\ . \tag{17}$$

The friction coefficient between the teeth in direct contact is assumed to be constant [4,5].

The hydrodynamic sliding friction force, F_{hf}, obtained by the half-Sommerfeld condition, is expressed as [11]

$$F_{hf} = \frac{\pi b \eta_o u_s}{2}\sqrt{\frac{R}{h}} \tag{18}$$

where u_s is the sliding velocity of the mating gears expressed as

$$u_s = u_p - u_g\ . \tag{19}$$

The moment arms of the friction forces F_{ef} and F_{hf} acting along the OLOA direction continue to change as meshing progresses (Fig. 3). The moments of the friction forces acting on the pinion and gear are

$$\begin{aligned}
&T_{efp} = (F_{ef}\sin\theta_{fp})r_{cp}\\
&T_{hfp} = (F_{hf}\sin\theta_{fp})r_{cp}\\
&T_{efg} = (F_{ef}\sin\theta_{fg})r_{cg}\\
&T_{hfg} = (F_{hf}\sin\theta_{fg})r_{cg}\\
&,where\\
&\theta_{fp} = \frac{\pi}{2} - \theta_{fcp},\ \theta_{fcp} = arctg(\frac{r_p}{\overline{B_1C}})\\
&\theta_{fg} = \frac{\pi}{2} - \theta_{fcg},\ \theta_{fcg} = arctg(\frac{r_g}{\overline{B_2C}})\\
&r_{cp} = (\overline{B_1C}^2 + r_p{}^2)^{\frac{1}{2}},\ r_{cg} = (\overline{B_2C}^2 + r_g{}^2)^{\frac{1}{2}}
\end{aligned} \tag{20}$$

where r_{cp} and r_{cg} are the distance from the center to the contact point of the pinion and gear, respectively.

As the friction forces change direction at the pitch point ($s = s_p$), the sign of the torque (T_{efp} and T_{efg}) caused by the direct contact friction force (F_{ef}) should change when the contact point passes the pitch point during meshing. However, because hydrodynamic friction forces are expressed as a function of the sliding velocity, which itself changes sign at the pitch point, the sign of the torque (T_{hfp} and T_{hfg}) caused by the hydrodynamic friction force (F_{hf}) is adjusted automatically.

3. Parametric study

Table 1 shows the dimensions of an identical gear pair used in previous research [7, 15-17] for comparison. The reference parameters were selected to be average mesh stiffness, 462.1×10^6 N/m; contact ratio, 1.75; tooth mesh damping ratio, 0.09; input torque, 150 Nm; ambient dynamic viscosity, 0.052 Pa-s (mineral oil at 45°C); average surface roughness (h_{min}), 2 μm [20]; and Coulomb friction coefficient, 0.05 [21].

To detect jump phenomena, sweeps with increasing and decreasing speeds were performed at a constant ratio for a wide range of speeds straddling the first

Table 1. Gear dimensions.

Number of teeth	50
Module (m)	0.003
Pressure angle (deg.)	20
Face width (m)	0.02
Modulus of elasticity (N/m^2)	$207x10^9$
Density (kg/m^3)	7600
Base radius (m)	0.07047
Backlash (2b) (m)	$400x10^{-6}$
Mass (kg)	2.8
Mass moment of inertia ($I_1=I_2$) (kgm^2)	$7.875x10^{-3}$

natural frequency. To obtain stable data after a speed change, 1×10^5 samples were discarded before averaging was performed. The time step was 1×10^{-5} s for all conditions.

The RMS of the DTE (RDTE) and the oscillating components of the DTE (ODTE) at a specific constant speed are defined as

$$RDTE=\sqrt{\frac{1}{N}\sum_{i=1}^{N}(DTE_i)^2}$$
$$ODTE=\sqrt{\frac{1}{N}\sum_{i=1}^{N}(DTE_{i+1}-DTE_i)^2}, \quad (21)$$

where $DTE_i = r_p\theta_p(t_i) - r_g\theta_g(t_i)$ and N is the total number of time steps used for averaging, which was 2×10^4 in this study.

Four different analysis models were simulated to identify the effects of the squeeze film and friction force on the gear pair dynamic behavior: direct contact without friction (DNF), direct contact with friction (DWF), mixed (direct and hydrodynamic) contact without friction (MNF), mixed contact with friction (MWF). For direct contact models (DNF and DWF), hydrodynamic force (F_{hn}) was neglected in Eq. (2). For models without friction (DNF and MNF), friction forces (F_{ef} and F_{hf}) were adjusted as zero in Eq. (20). The solutions were obtained by using direct time-domain numerical integration (fifth-order Runge-Kutta algorithm). The state parameters of the four different models were compared for various values of lubricant viscosity, film width, Coulomb friction coefficient, and backlash.

The pressure distribution across the film width was examined (Fig. 5) before examining the other state parameters. The shape of the pressure distribution across the film width was similar to that reported previously, and the peak value was of the same order [8, 19].

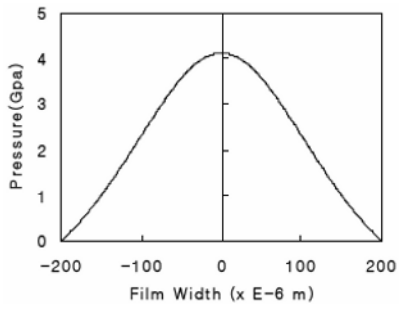

Fig. 5. Pressure distribution across the film width: viscosity 0.052Pa-s, film width 200 μm .

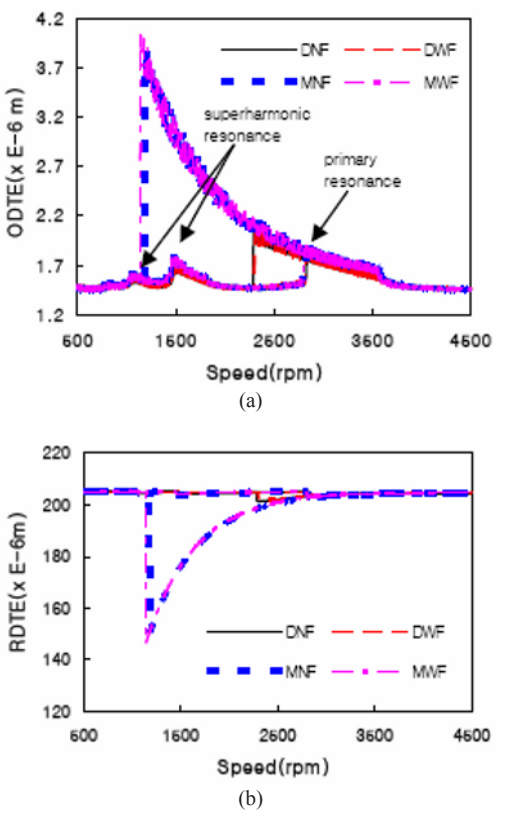

Fig. 6. Response of a gear pair system: (a) RDTE and (b) ODTE.

Fig. 6 shows the ODTE and RDTE as a function of rotation speed of the four different models. This figure shows the jump-up and jump-down phenomena at the primary resonance frequency as well as at the superharmonic frequency. The effect of friction on the rota-

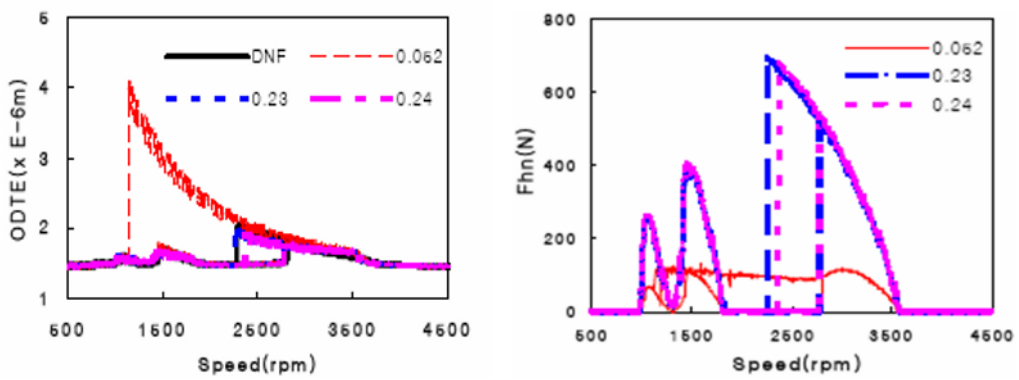

(a) (b)

Fig. 7. Dynamic response of the MWF model for various viscosities: (a) ODTE and (b) hydrodynamic normal force (F_{hn}).

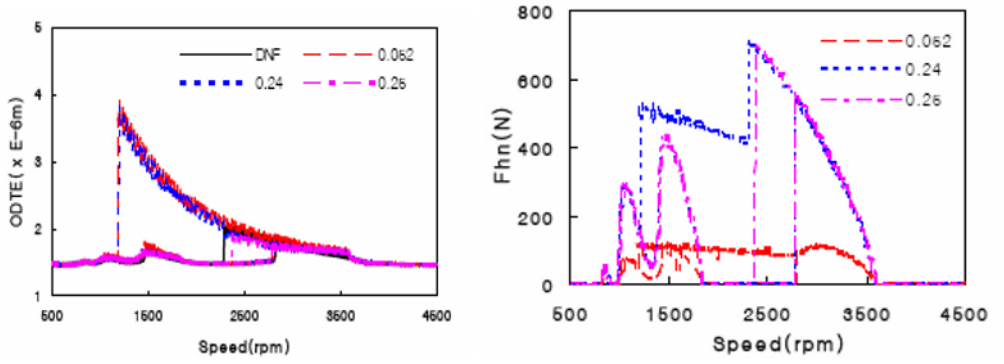

(a) (b)

Fig. 8. Dynamic response of the MNF model for various viscosities: (a) ODTE and (b) hydrodynamic normal force (F_{hn}).

tional motion is very small. The overlap range (multiple solution regimes) increases dramatically in the case of the mixed model. Thus, the squeeze effect increases the nonlinear behavior. This seems reasonable because the tooth meshing force due to the squeeze effect was considered even when teeth were separated in the mixed model, unlike the direct-contact model in which the tooth meshing force was assumed to be zero when the teeth were separated.

Although the lubricant viscosity was assumed to have the value of atmospheric pressure, the overlap range was very much wider than the experimental result [7], which was probably due to an inappropriate reference viscosity. As the oil viscosity can increase more than 100 times the ambient value due to high contact pressure [10, 19], the analysis was conducted for various viscosity levels to find a reasonable value to give behavior similar to the experimental results.

Figs. 7 and 8 show that the dynamic behavior of the gear was greatly affected by the lubricant viscosity. The overlap range decreased as the viscosity increased due to the increased damping effect of the squeeze film, and the overlap range decreased sharply at a specific critical value. The critical viscosity value was lower when the friction force was included, which indicated that the damping effect was less if friction was not included. Based on previous experimental results [7], a reference viscosity of 0.25 Pa-s was selected for further analyses. This value is about 5 times the ambient value, and is in a reasonable range.

Film width ($2a$ in Fig. 2) for calculating the hydrodynamic force due to the squeeze effect is the key factor for the hydrodynamic model.

Hence, ODTE values for the MWF model were compared for various film widths as a function of rotational speed (Fig. 9). It is clear that the gear behavior was affected strongly by film width. A small film width increased the overlap range to a much greater

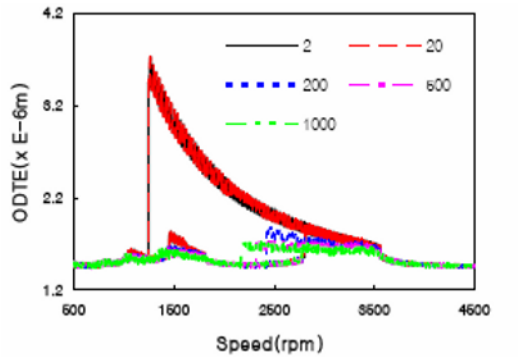

Fig. 9. ODTE of the MWF model for various film widths (μm).

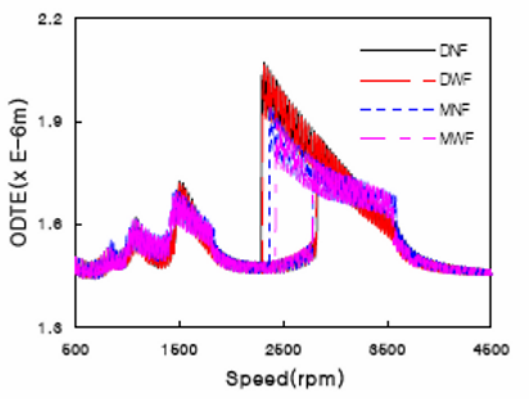

(a)

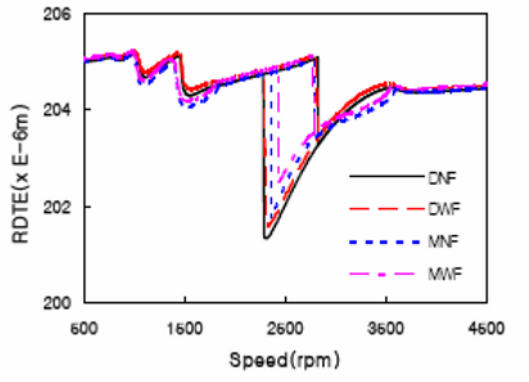

(b)

Fig. 10. Dynamic responses of various models as a function of speed: (a) ODTE and (b) RDTE.

extent than larger film widths. Thus, large damping by a larger film width would decrease the nonlinear behavior, although the squeeze effect increased nonlinear behavior.

Although viscosity and film width were treated as

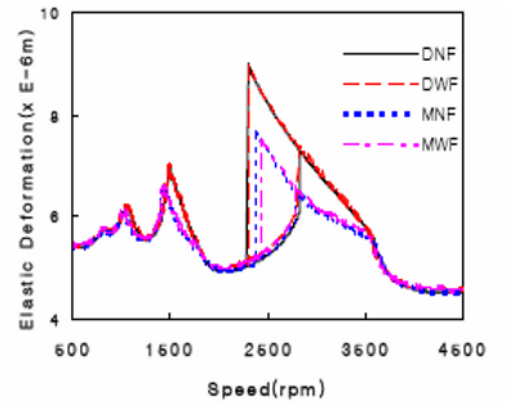

(a)

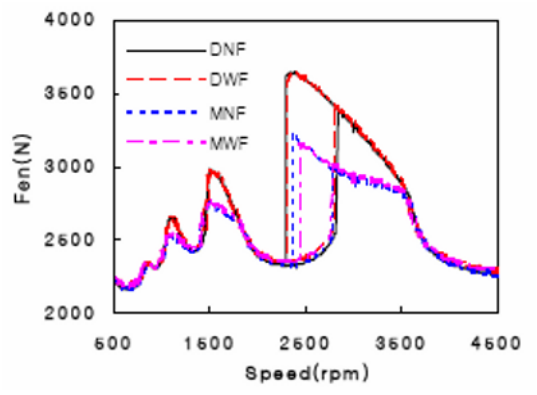

(b)

Fig. 11. Dynamic responses of various models as a function of speed: (a) elastic deformation (b) direct contact normal meshing force (F_{en}).

independent parameters in this study, the film width will be affected by the viscosity, and the viscosity will be the primary parameter affecting the hydrodynamic behavior of a gear system. Based on previous experimental results [7], the reference film width was set to 200 μm for further analyses.

Fig. 10 shows the ODTE and RDTE as a function of rotational speed for the various models with the reference parameters. In all models, the speed of tooth separation, jump-up, jump-down, and the softening behavior were almost the same. Inclusion of the friction decreased the RDTE slightly in both the direct-contact and mixed models. It seems that the relatively simple direct-contact models can be used for investigating general rotational nonlinear behavior of a spur gear pair by selecting the appropriate system parameters. As the experimental results [7] did not clearly show the lubrication conditions, comparisons of these

data with the results of this study may have some limitations.

Fig. 11 shows the elastic deformation and normal tooth contact forces by direct contact in the various models as a function of rotational speed. Due to fluid film damping, the deformations and tooth contact forces of the mixed models were smaller than those of the direct-contact models.

Fig. 12 shows the tooth gap (fluid film thickness) formed by tooth separation. Tooth separation occurs around the primary resonance frequencies as well as the 2nd and 3rd superharmonic frequencies. Although tooth separation occurred only as for the speed-decreasing phase near the primary natural frequency, it occurred for both increasing and decreasing phases around the superharmonic frequencies. In these regimes, tooth separation as well as direct contact repeated, and this behavior caused severe vibration. On the other hand, the teeth maintained contact without separation in the other regimes. The peak magnitude of the hydrodynamic normal force (F_{hn}) due to the squeeze effect was about one fifth of the elastic force (F_{en}) due to elastic deformation by direct contact, and was sufficiently large that it could not be disregarded. Forces due to the entraining velocity and the hydrodynamic friction were about two orders smaller than F_{en} over the whole speed range, and are not shown here.

While Brancati et al. [13, 14] included only the squeeze term in their study, Theodossiades et al. [11, 12] assumed the contribution to hydrodynamic force due to squeeze is very small compared with that due to entraining motion since the squeeze film velocity is much smaller than the entraining speed. However, hydrodynamic force is not a function of squeeze film velocity ($\dot{x}$) and entraining speed ($\bar{u}$) only, but is that of $a\bar{u}$ *and* $R\dot{x}$ as in Eq. (12). Hence, it is reasonable not to assume the contribution to hydrodynamic force due to squeeze is negligible than that due to entraining motion. Because Theodossiades et al. and Brancati et al. analyzed idle rattle motion at relatively lower speeds than this study, all the analytical results

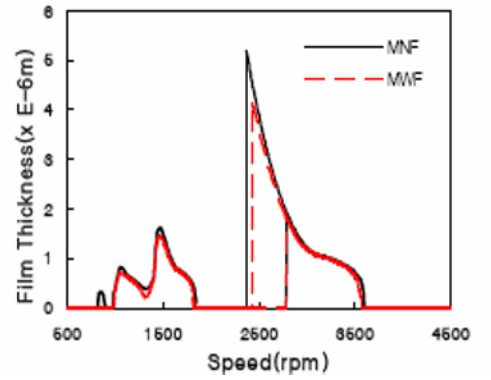

(a)

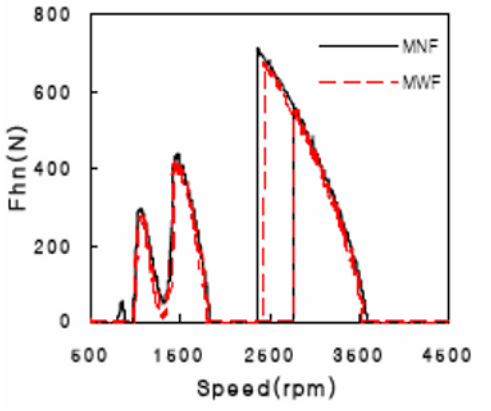

(b)

Fig. 12. Film thickness and hydrodynamic normal force (F_{hn}) of the mixed model: (a) film thickness and (b) F_{hn}.

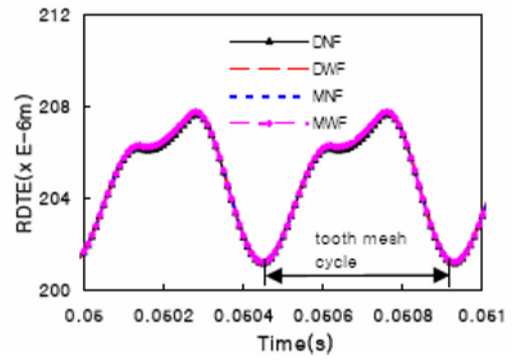

(a)

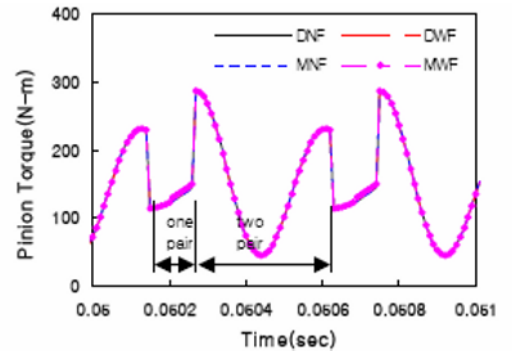

(b)

Fig. 13. RDTE and pinion torque as a function of time of various models at 2500 rpm, lower branch.

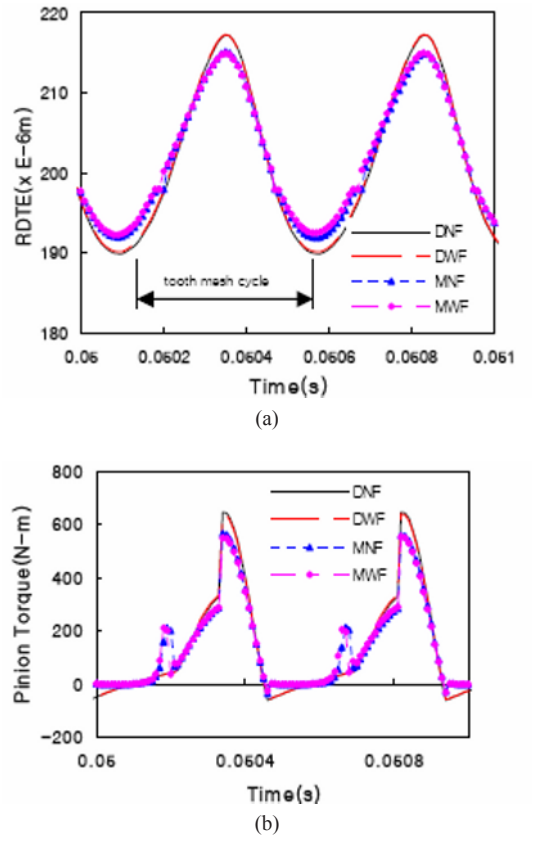

(a)

(b)

Fig. 14. RDTE and pinion torque as a function of time of various models at 2500 rpm, upper branch.

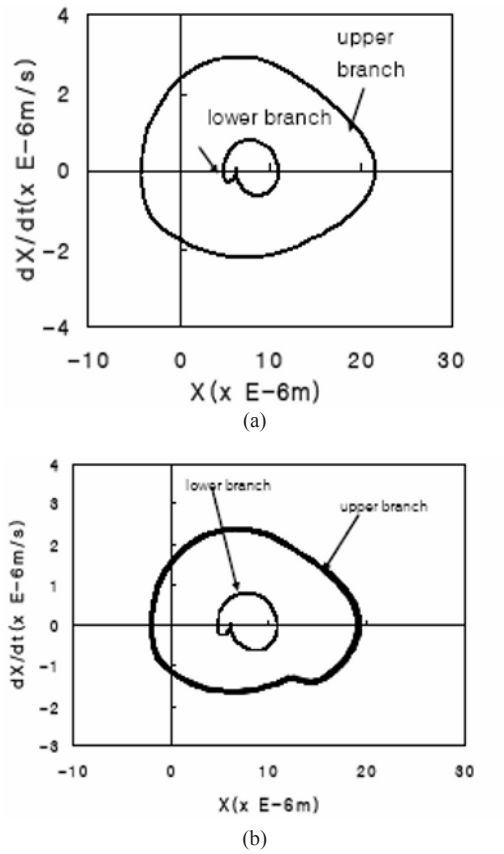

(a)

(b)

Fig. 15. Phase plane of (a) DNF model and (b) MWF model.

presented in this study should be verified through further experimentation.

Figs. 13 and 14 show the RDTE and pinion torque as a function of time for the various models at 2500 rpm where the system had multiple solutions. During increases in speed (lower branch), the RDTE was always greater than the backlash (200 μm), and no tooth separation occurred. The pinion torque varied due to the change of tooth mesh pairs between one and two, and caused slight variations in the RDTE profile.

The overall trends of the four models were almost the same. The magnitudes of the RDTE and the pinion torque of the mixed models were less than those of the direct-contact model due to the damping effect of the squeeze film.

Significant torque variations induced by the changes in friction forces around the pitch point have been reported previously [1, 2]. However, there was just a slight torque variation around the pitch point in this study, which seemed to have been due to the relatively small friction forces that were much lower than the normal forces.

During decreases in speed (upper branch), the RDTE fluctuated between values of less than 200 μm and over 215 μm. Induced by a large elastic deformation, the pinion torque varied over a wide range of values. Due to the driving torque, the pinion torque had values less than zero while the teeth were separated, and this tendency was more prominent in the direct-contact models that do not have a squeeze film damping area. Overall, the trends of the four models were almost the same except for the torque of the mixed models because of the squeeze force when the teeth came into contact.

Fig. 15 shows the phase plans of the DNF and MWF models. Due to tooth separation and wide fluctuations during decreases in speed, the loci of the upper branch were much larger than those of the lower branch. The loci of the MWF model showed more fluctuation than the DNF model, but were very simple and stable.

Fig. 16 shows the ODTE of the MWF model for

various backlashes as a function of rotational speed. The DTE decreased with increases in backlash, and the overall behavior was similar. Although the backlash varied over a wide range, the elastic deformation and tooth gap did not vary much and are not shown here. The different backlash values had very little effect on the dynamic behavior of gear systems.

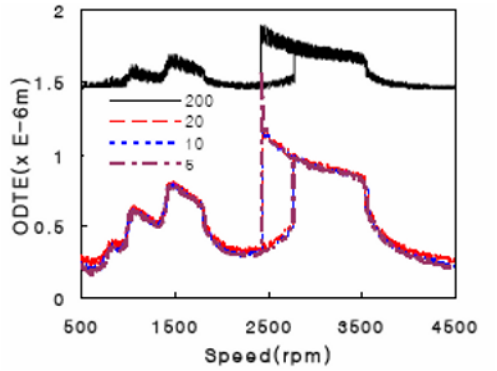

Fig. 16. ODTE responses of MWF model for various backlashes (μm).

Fig. 17 shows the ODTE and RDTE of the MWF model for various friction coefficients as a function of rotational speed. It is clear that friction coefficient had little effect on the rotational dynamic behavior of the gear system.

Fig. 18 shows the ODTE and RDTE of the MWF model for various torques as a function of rotational speed. The RDTE and ODTE decreased as the torque decreased, but the overlap range increased. A light load is likely to separate the teeth.

As the ODTE is the main source of noise and vibration in gear systems [22], and elastic deformation and ODTE decrease as viscosity increases (Figs. 7 and 8), the dynamic responses were simulated for various viscosity values even 100 times higher (5.2 Pa-s) than the ambient value (Fig. 19). The ODTE and RDTE decreased as the viscosity increased. However, the overlap range was not a function of viscosity, but had a maximum value for any specific viscosity. The hydrodynamic force stimulated the nonlinear behavior to

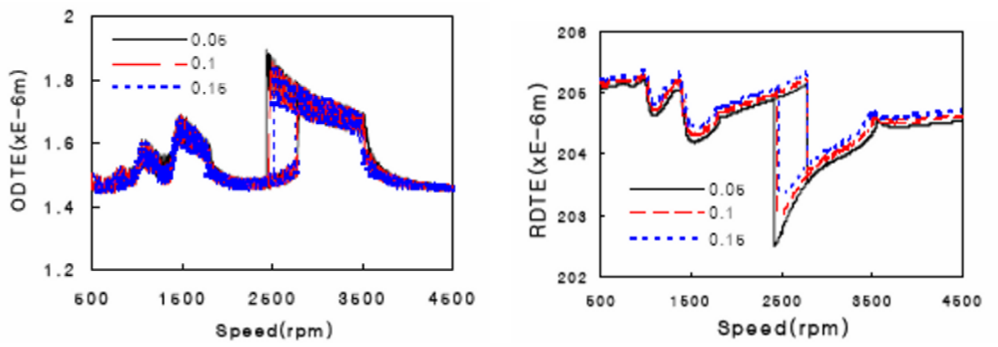

(a) (b)

Fig. 17. Dynamic responses of MWF model for various friction coefficients: (a) ODTE and (b) RDTE.

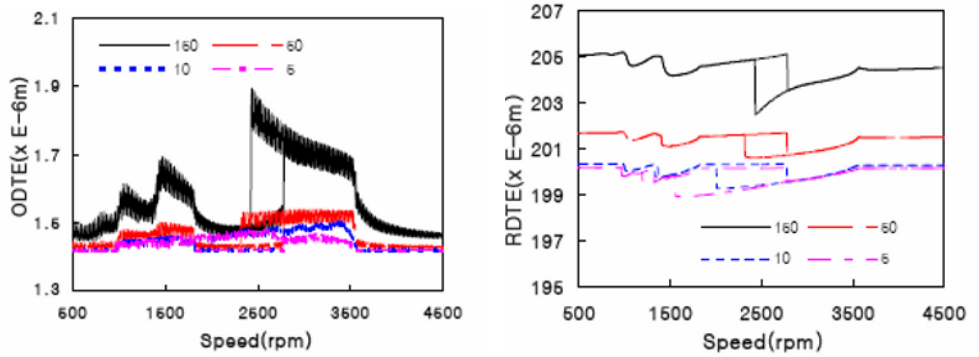

(a) (b)

Fig. 18. ODTE and RDTE responses of the MWF model for various torques (N-m).

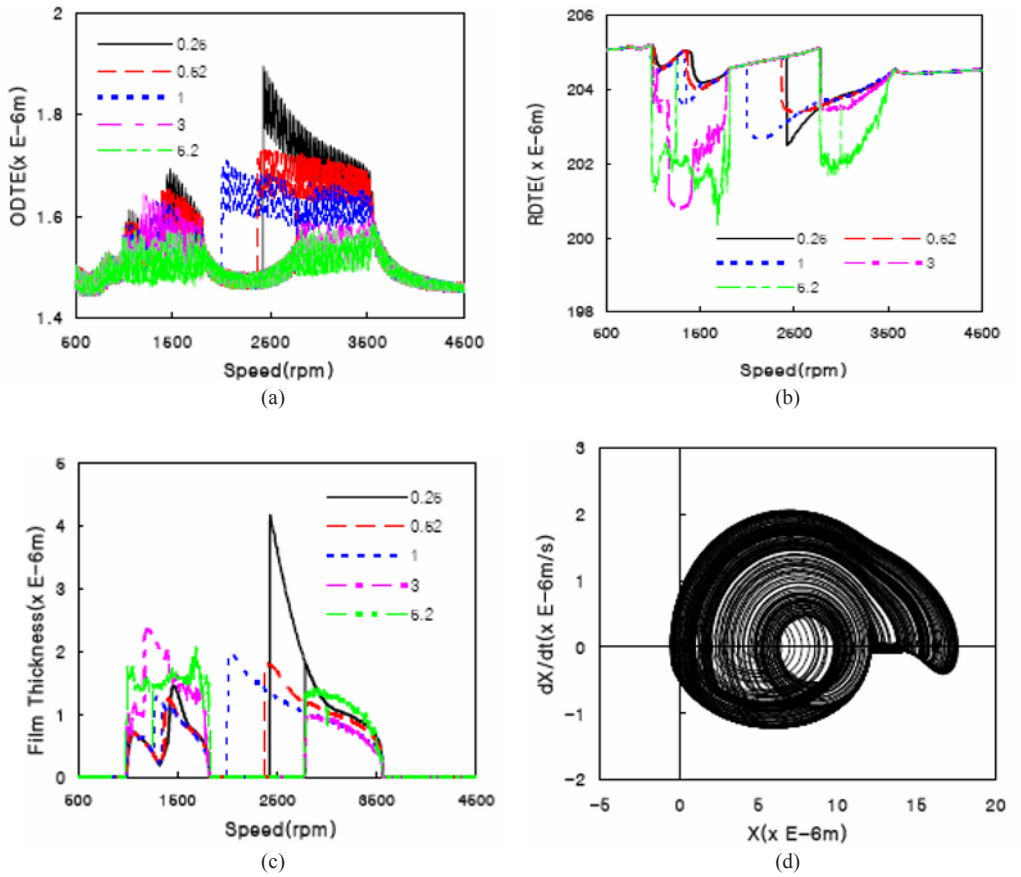

Fig. 19. Dynamic responses of the MWF model for various viscosities (Pa-s): (a) ODTE, (b) RDTE, (c) film thickness, (d) phase plane (5.2 Pa-s, 1700 rpm).

increase the overlap range as well as to decrease the overlap range by damping. It is expected that noise and vibration could be minimized by maintaining the viscosity at an optimal value. Gear pairs exhibited chaotic behavior at very high viscosity.

4. Conclusions

Four different analysis models were simulated to identify the effects of hydrodynamic force and friction force on the dynamic behavior of gear pairs. Nonlinear behavior over a wide range of speeds was analyzed in a direct-contact elastic deformation model including the hydrodynamic effect and friction force. The state parameters of the models were compared for various values of lubricant viscosity, film width, Coulomb friction coefficient, and backlash. Inclusion of the hydrodynamic effect facilitated nonlinearity and damping, and decreased elastic deformations and tooth reaction forces. Viscosity had a strong effect on the behavior of gear pair systems, but friction had very little effect on gear pair torsional behavior.

Overall, the nonlinear behaviors of various models over a wide range of speeds were similar to each other. The overall nonlinear behavior over a wide range of speeds can be analyzed by the direct-contact model rather than the more complex hydrodynamic model if parameter values are chosen appropriately. However, the hydrodynamic model is necessary for detailed time data analysis because the squeeze effect forces cannot be detected by the direct-contact model. All the analytical results presented in this study should be verified through further experimentation.

Acknowledgment

This paper was supported by Wonkwang University in 2008.

References

[1] M. Vaishya and R. Singh, Analysis of Periodically Varying Gear Mesh Systems with Coulomb Friction Using Floquet Theory, *J. of Sound and Vibration*, 243 (3) (2001) 525-545.

[2] M. Vaishya and R. Singh, Sliding Friction-Induced Non-Linear and Parametric Effects in Gear Dynamics, *J. of Sound and Vibration*, 248 (4) (2001) 671-694.

[3] S. He, R. Gunda and R. Singh, Effect of Sliding Friction on the Dynamics of Spur Gear Pair with Realistic Time-Varying Stiffness, *J. of Sound and Vibration*, 301 (2007) 927-949.

[4] S. He, S. Cho and R. Singh, Prediction of Dynamic Friction Forces in Spur Gears Using Alternate Sliding Friction Formulations, *J. of Sound and Vibration*, 309 (2008) 843-851.

[5] I. Howard, S. Jia and J. Wang, The Dynamic Modeling of a Spur Gear in Mesh Including Friction and a Crack, *Mechanical System and Signal Processing*, 15 (5) (2001) 831-853.

[6] P. Velex amd P. Sainsot, An Analytical Study of Tooth Friction Excitations in Errorless Spur and Helical Gears, *Mechanism and Machine Theory*, 37 (2002) 641-658.

[7] A. Kahraman and G. W. Blankenship, Effect of Involute Contact Ratio on Spur Gear Dynamics, *Transactions of the ASME, J. of Mechanical Design*, 121 (1999) 112-118.

[8] R. Larsson, Transient Non-Newtonian Elastohydrodynamic Lubrication Analysis of an Involute Spur Gear, *Wear*, (1997) 67-73.

[9] Y. Wang, H. Li, J. Tong and P. Yang, Transient Thermoelastohydrodynamic Lubrication Analysis of an Involute Spur Gear, *Tribology*, 37 (2004) 773-782.

[10] P. Kumar, P. K. Saini and P. Tandon, Transient Elastohydrodynamic Lubrication Analysis of an Involute Spur Gear Using Couple-Stress Fluid, *Proc. IMechE Part J: J. Engineering Tribology*, 221 (2007) 743-754.

[11] S. Theodossiades, O. Tangasawi and H. Rahnejat, Gear Teeth Impacts in Hydrodynamic Conjunctions Promoting Idle Gear Rattle, *J. of Sound and Vibration*, 303 (2007) 632-658.

[12] O. Tangasawi, S. Theodosiades and H. Rahnejat, Lightly Loaded Lubricated Impacts: Idle Gear Rattle, *J. of Sound and Vibration*, 308 (2007) 418-430.

[13] R. Brancati, E. Rocca and R. Russo, A Gear Rattle Model Accounting for Oil Squeeze Between the Meshing Gear Teeth, *Proc. IMechE Part D: J. Automobile Engineering*, 219 (2005) 1075-1083.

[14] R. Brancati, E. Rocca and R. Russo, An Analysis of the Automotive Driveline Dynamic Behavior Focusing on the Influence of the Oil Squeeze Effect on the Idle Rattle Phenomenon, *J. of Sound and Vibration*, 303 (2007) 858-872.

[15] G.-J. Cheon, Nonlinear Behavior Analysis of Spur Gear Pairs with a One-Way Clutch, *J. of Sound and Vibration*, 301 (2007) 760-776.

[16] G.-J. Cheon, Effects of a One-Way Clutch on the Nonlinear Dynamic Behavior of Spur Gear Pairs under Periodic Excitation, *J. of Mechanical Science and Technology*, 20 (7) (2006) 941-949.

[17] R. G. Parker, S. M. Vijayakar and T. Imajo, Non-Linear Dynamic Response of a Spur Gear Pair: Modeling and Experimental Comparisons, *J. of Sound and Vibration*, 237 (3) (2000) 435-455.

[18] D. Dowson and G. R. Higginson, *Elasto-Hydrodynamic Lubrication*, Pergamon Press, New York, (1977).

[19] W. J. Bartz, *Lubrication of Gearing, Mechanical Engineering Publications*, London, (1993).

[20] B. R. Hohn, K. Michaelis and F. Kopatsch, Determination of Film Thickness, Pressure and Temperature in Elastohydrodynamic Lubrication in the Past 20 Years in Germany, *Proc. IMechE Part J: J. Engineering Tribology*, 215 (2001) 235-242.

[21] J. Castro and J. Seabra, Coefficient of Friction in Mixed Film Lubrication: Gears Versus Twin-Discs, *Proc. IMechE Part J: J. Engineering Tribology*, 221 (2007) 399-411.

[22] J. D. Smith, *Gear Noise and Vibration*, Marcel Dekker, New York, (1999).

Cheon Gill-Jeong received his B.S. in Mechanical Engineering from Seoul National University (SNU), Korea, in 1981. He then received his M.S. and Ph.D. degrees from SNU in 1983 and 1988, respectively. He served as a senior research engineer at Seoul National University Hospital and Daewoo Heavy Industry for several years. Dr. Cheon is currently a Professor at the Division of Mechanical Engineering at Wonkwang University in Iksan, Korea. His research interests include dynamics, tribology, and design engineering.